Automatic Detection for Day and Night Time Dust Storms Using MODIS bands.

Esam El-ossta
Higher Institute of Comprehensive Vocations, Gharyan .

الخلاصة :

تعتبر العواصف الرملية واحدة من المخاطر الطبيعية التي ارتفعت وتيرتها في السنوات الأخيرة فوق كل من الصحراء الكبرى، واستراليا، وشمال الصين. لذلك كان من المهم دراسة هذه الظاهرة لمعرفة مسبباتها وطريقة تحركها وكذلك تأثيراتها الإشعاعية.

تعتبر الأقمار الاصطناعية من أهم الطرق المستخدمة في مراقبة العواصف الرملية، إلا أن استخدامها فوق الأسطح الرملية يشوبه بعض العيوب، وذالك لأن العواصف الرملية والأسطح الرملية تتشابه في العديد من الخصائص. كذلك قام العديد من الباحث بدراسة مشكلة اكتشاف العواصف الرملية من صور الأقمار الاصطناعية خلال فترات النهار على مناطق مختلفة من الأرض مثل الصين، واستراليا، وأمريكا، وكذلك في شمال أفريقيا مستخدمين بيانات مختلفة من هذه الصور. إلا أن هناك عدد بسيط من الدراسات قامت بدراسة اكتشاف العواصف الرملية من صور الأقمار الاصطناعية خلال فترة الليل. العنصر الرئيسي في هذا البحث هو استخدام لغة الذكاء الاصطناعي مع استخدام تقنية درجة حرارة السطوع المستخلصة من صور الأقمار الاصطناعية باستخدام الحزمة 31 وأيضاً استخدام تقنية الاختلاف في درجات الحرارة باستخدام بيانات مؤسسة (MODIS) والتي تستقبل بياناتها من القمرين تيرا وأكوا لتصميم طريقة جديدة لاكتشاف العواصف الرملية خلال فترتي الليل والنهار. نتيجة هذا البحث أظهرت أن هذه الطريقة تستطيع استخلاص العواصف الرملية من صور القمرين تيرا وأكوا خلال فترتي الليل والنهار بالإضافة إلى إمكانية استخلاص العواصف من مختلف سطوح الأرض.

Abstract :

Dust storms are one of the natural hazards whose incidence has increased in the recent years over Sahara desert, Australia and northern China. Thus, it is important to know the causation, movement and radiation effects of dust storms. Satellite remote sensing is the most common method for monitoring Dust Storms but its use over sandy ground is still limited as they have similar characteristics. Many researchers have studied the detection of dust storms during daytime in a number of different regions of the world including China, Australia, America, and North Africa using a variety of satellite data. However, there have been fewer studies for detecting dust storms at night. The key elements of this study are to use a back-propagation artificial neural network with Brightness Temperature of band 31 and four Brightness Temperature Differences calculated using data from the Moderate Resolution Imaging Spectroradiometers on the Terra and Aqua satellites to develop a method for detecting dust storms during both day and night. Results have shown that the method can detect dust storms at both day and night and also over different land surfaces.

Keywords: Dust Storms; MODIS; Sahara; Brightness Temperature Difference; Satellite remote sensing.

I. INTRODUCTION :

Dust storms are a type of natural disaster occurring in many parts of the word, including north Africa, northern China, Australia, the Arabian desert, and Turkmenistan, which have worsened during the last decade, affected by changes of climate [1, 2]. Dust storms increase air pollution, impact on urban areas and farms as well as affecting ground and air traffic [3]. They cause damage to human health, reduce the temperature, reduce visibility [4] and cause damage to communication facilities [5]. Saharan dust storms, for example, caused by a combination of dry conditions and strong winds, can transport sand over large areas of the Earth to reach as far as the north of Europe, parts of Asia and North America [3]. While dust storms are only one of many natural hazards, monitoring and tracking them has become very important in recent years to help governments to alleviate the consequences of these storms. At the present time

there are only two main methods available for monitoring dust storms. The first is ground based measurements and the second is satellite based remote sensing technology, in which interest is increasing [4]. This is because ground based measurements cannot meet the requirements of monitoring and tracking dust storms very well.

Satellite remote sensing is likely to become the primary approach for the detection of dust storms [1], because there are many potential advantages to using this technology, including flexible coverage of wide areas and continuous or frequent monitoring of the earth. At the same time, satellite remote sensing is indirect, and the uses of true-colour images, aerosol optical thickness (AOT), and deep blue algorithm, for example, are limited. However, in principle, the severity of dust storms, the areas they affect and changes in intensities can be monitored using remotely sensed images [4]. This is why many researchers have proposed methods to distinguish dust storms from clouds, ground and water surfaces using images in many different spectral bands from instruments, such as MODIS, MERIS, AVHRR, TOMS, SeaWiFS [1, 2, 4-6]. However, the detection of dust storms is complicated because they share some characteristics with clouds, which can make it very difficult to distinguish them in some spectral bands [2]. Furthermore, the characteristics of dust storms and ground sand are similar, which makes it difficult to discriminate between them.

In this study we have concentrated on MODIS (Moderate Resolution Imaging Spectroradiometer) data provided by the NASA Terra and Aqua satellites (passing north to south across the equator in the morning and south to north across the equator in the afternoon, respectively) because these provide data in 36 spectral bands. This potentially provides more opportunities for developing techniques for the detection of dust storms than data from some other satellites. The following paragraphs discuss previous work and its limitations.

Qu et al. [1] proposed a method for dust storm detection based on the Normalised Difference Dust Index (NDDI) defined in equation (1).

$$NDDI = (b7 - b3)/(b7 + b3) \quad (1).$$

Where b7and b3 are the reflectances in MODIS bands 7 and 3 (2.13μm and 0.469μm), respectively. Even though, this method was useful for the detection of dust storms over non sandy ground, it did not provide good results over sandy ground like the Sahara desert, when it was implemented by authors of this paper even when enhanced using the brightness temperature from band 31 (11.03μm). It seems to successfully use this technique over surfaces like the Sahara it is likely that extra bands will need to be included. Mei et al. [4] have used the BTD between bands 31 (11.03μm) and 32 (12.02μm) and a 0K threshold for dust storm detection during both day and night in the north west of China in 2006. However this did not provide the desired performance because some clouds were still detected. Hence they used an NDDI technique to remove clouds during the day. At the same time the Brightness Temperature of band 31 was used to separate dust storm and cloud during the night using thresholds greater than 263K and less than 280K. Although, this method was very effective for the detection of dust storms over north western China, it was less effective for the detection of dust storms over the Sahara desert when this was tried by the present authors.

The MODIS bands 20, 25, 29, 31 and 32 (3.7μm, 4.6μm, 8.6μm, 11μm and 12μm) are the thermal infrared channels most commonly used for dust storm detection. The brightness temperature differences between pairs of these bands can be used to identify dust storm from other objects in MODIS images. The brightness temperature difference between 11μm and 12 μm have been employed in many dust storm detection schemes [7]. Since, for the same radiance, the brightness temperature of a dust storm at 12μm is normally higher than the brightness temperature at 11μm, the values of dust storm in the brightness temperature difference between 11μm and 12μm will be negative and most of the other objects will be around zero or positive [8]. Also the water vapour absorption at 8.6μm is higher than at 11μm [2]. For this reason the brightness temperature difference between 8.6μm and 11μm will be positive, the BTD (11-12) < 0 and BTD (8.6-11) > threshold for detection dust storms at both day and night times [2]. The three brightness temperature differences BTD (3.7-11), BTD

(8.6-11) and BTD (12-11) from four MODIS bands are used to develop the Thermal Infrared Integrated Dust Index (TIIDI) technique to detect a dust storm over sandy, vegetation, or water surfaces [8]. Furthermore, the two brightness temperature differences BTD (4.6-11) and BTD (11-12μm) from three MODIS bands and the NDDI technique are used to detect dust storms over the Sahara desert [9].

Neural Networks have been widely used to classify data for vegetation and other land cover obtained from satellites. Rivas-Perea et al. [10] made a comparison between Probabilistic Neural Network (PNN) and Maximum Likelihood (ML) based methods for Dust Aerosol Detection using MODIS multispectral data. Five selected features were used for both methods: individual bands 1 (0.645μm), 4 (0.555μm) and 3, BTDs from bands 32 and 31, and from bands 20 (3.75μm) and 29 (8.55μm). The results of this comparison showed better detection of the dust storm using the PNN than the ML with PNN detecting 77% of dust compared with 52% with ML. However, when the Neural Network method with the same features was implemented on data from the Sahara it was less effective. The aim of this work is to apply a back propagation artificial neural network approach to attempt to generate an automated system that can detect dust storm at both day and night over different earth surfaces.

Section II summarises the data used in this study, Section III explains the methodology used in this work for dust storm detection and section IV shows results from the implementation of this work over different surface for both day and night.

II. DATA :

MODIS level1B data obtained from both Terra and Aqua satellites were used for training and testing the dust storm detection algorithm. Both satellites provide data from 36 channels divided into three groups according to its resolution. Bands 1 (0.645μm) and 2 (0.856μm) have 250m resolution, bands 3 to 7 have 500m resolution, and bands 8 (0.413μm) to 36 (14.24μm) have 1km resolution. Furthermore, bands 1 to 19 (0.94μm) and 26 (1.38μm) are solar reflectance bands (SRBs)

whereas the others are emissive bands. The MODIS satellites can make a complete orbit in 24 hours and provide one MODIS image every five minutes [1, 4, 11].

A number of MODIS recorded dust storm events were selected from the NASA Earth Observatory (NEO) for investigation in this paper, captured by either Terra or Aqua satellites for different regions of the earth at the dates and times listed in Table I. The first 25 rows of Table I are described as images containing dust storms by the NEO. The final two rows in Table I are included to provide vegetation and snow references and do not contain dust storm data.

These data were downloaded from Level 1 and Atmosphere Archive and Distribution system website. Then regions containing dust storms were identified and used at later stages for subjective comparison with the NN output.

table I, the image data sets used in this study .

MODIS Data	Date	Time(GMT)	Location	Satellite
19	10/11/2001	10:45	Algeria	Terra
3	02/02/2003	11:20	Mediterranean see	Aqua
10	28/05/2004	12:00	Sahara	Aqua
5	12/02/2005	14:50	Atlantic Ocean	Aqua
9	01/03/2005	12:20	Libya	Aqua
6	12/05/2005	23:35	Saudi Arabia	Aqua
2	13/05/2005	10:35	Saudi Arabia	Aqua
4	13/05/2005	08:00	North of Saudi Arabia	Aqua
7	18/07/2005	13:40	Sahara	Aqua
1	19/07/2005	12:45	Sahara	Aqua
8	14/12/2005	12:20	Sahara	Aqua
20	23/02/2006	09:15	Libya	Terra
11	24/02/2006	11:30	Sahara	Aqua
23	24/02/2006	08:20	Egypt	Terra
21	01/01/2008	11:10	Morocco	Terra
27	07/01/2008	11:50	UK	Terra

26	08/06/2008	10:30	Sahara	Terra
22	03/08/2008	11:15	Spain	Terra
12	22/04/2010	13:20	Sahara	Aqua
24	24/07/2010	08:05	Red Sea	Terra
25	11/11/2010	03:15	Eastern China	Terra
16	28/02/2011	07:40	North west of China	Aqua
17	02/03/2011	07:30	North west of China	Aqua
13	26/03/2011	09:50	South of Saudi Arabia	Aqua
18	08/04/2011	11:00	South west UK	Terra
14	26/05/2011	11:00	Red sea	Aqua
15	25/07/2011	17:45	China	Aqua

II . METHOD :

A. THE FEATURE EXTRACTION METHOD :

The brightness temperature difference of BTD (3.7-11), BTD (4.6-11), BTD (8.6-11), BTD (11-12) and the brightness temperature of band 31 (BT31) were generated for all the downloaded images shown in Table I.

Windows of size 40×40 are used to extract pixel values for regions representing dust storms and non-dust storms. For each image different windows could be used to represent weak and strong dust storms, also dust storms over land or sea. For each window used a feature vector of size 1600 is used. The total number of windows used in this research is 100 (19 for dust storm, 20 for cloud, 16 for vegetation, 17 for Land, 18 for water and 10 for snow).

A feature vector is generated from the objects were extracted from the four BTD and BT31 to generate a feature vector. Table II illustrate some examples of trained data.

A feed-forward back propagation Neural Network technique is used for training and testing these data to identify pixel values of dust storms over different surfaces during both day and night. A total of 160000 samples, each comprising four BTD and one BT31 valued which were generated from all the

data listed in Table I. This comprises MODIS data chosen from different surface regions and for both day and night. These samples were randomly divided into two sets, the first 80% were used for training and the second 20% were used for testing the neural network performance. After completion of training, the neural network was applied to the test data with 100% accuracy. Further tests were carried out including an additional 90 sets with clearly visible dust storm boundaries, obtained in 2011. These were manually selected from the 150 classified as dusty data on NASA Earth Observatory.

table II sample of date uesd for training neural network .

BTD(3.7-11)	BTD(4.6-11)	BTD(8.6-11)	BTD(11-12)	BT 31	Class
31.3	11.1	-0.7	-2.1	286.6	1
25.3	7.1	-8.8	-2.2	287.0	1
46.5	22.2	1.5	2.1	272.9	0
4.8	2.1	-5.2	-0.	275.0	0

MODIS BTDs images contain regions of cloud, dust storm, land, water, snow, and vegetation. Ground truth data for dust storm and no dust storm were obtained by manual inspection of the true colour bands at day and band 31 at night because no other source of ground truth date was available. The performance of the neural network was evaluated using the performance metrics: 'True Positive Rate' (TPR), 'False Positive Rate' (FPR), 'Accuracy' (ACC), 'True Negative Rate' (TNR) and 'False Detective Rate (FDR).Figure 1 illustrates the structure of using feed-forward back propagation Neural Network technique. After the satisfaction of trained feed-forward back propagation Neural Network, the new technique was applied for hole dusty images comparing with manually dust stormdetection.

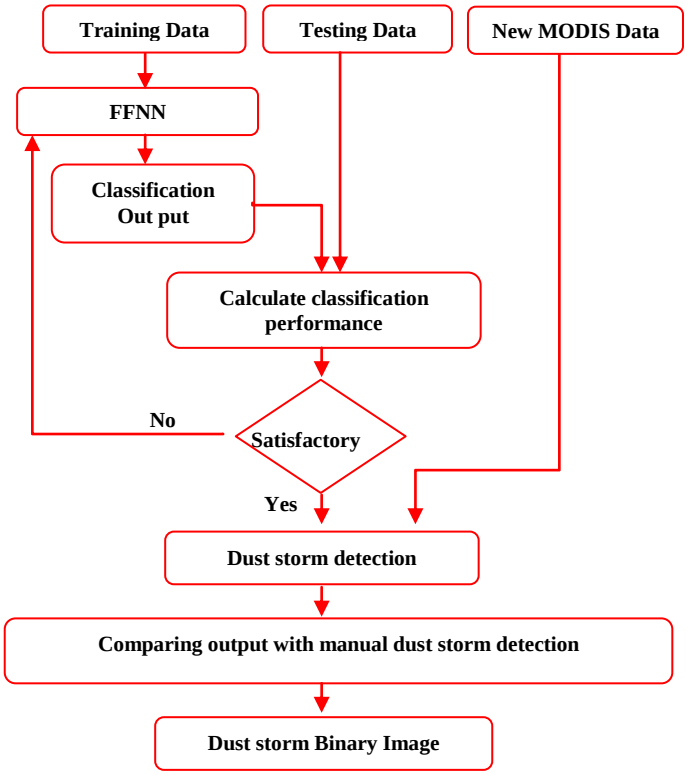

figure 1structure of using feed-forward back propagation neural network technique

II .RESULTS AND DISCUSSION :

The Neural Network based approach has been applied to the MODIS data listed in Table I and MODIS data of dust storms occurred on 2011. This includes data captured of dust storms over land, ocean and vegetation surfaces and during both day night. In the subsections which follow, the results obtained have been divided according to the four categories of surface: desert; vegetation; ocean water; and desert at night.

A. Desert Surfaces Results :

The trained neural network was applied to MODIS data in table I as well as all dust storms events occurred on 2011 and obtained over all desert surfaces and was found to detect over

all about 80% of the manually detected dust storm pixels. Table III illustrate the average result of detection dust storm over desert.

Table III the result of trained neural network over desert surface.

	TPR	FPR	ACC	TNR	FDR
Average	0.80	0.06	0.93	0.94	0.4

Figure 2a shows the true colour image of a dust storm event which occurred over Sahara on 18th of July 2005 captured by the Aqua satellite. Figure 3a shows the true colour image of a huge dust storm over the north of Saudi Arabia and south of Jordan on 13th of May 2005, also captured by the Aqua satellite. Figures 2b and 3b show the results from the dust storm detection algorithm for both events shown in figures 2a and 3a respectively, which illustrate the discrimination between dust storm and both cloud and desert and other land surfaces.

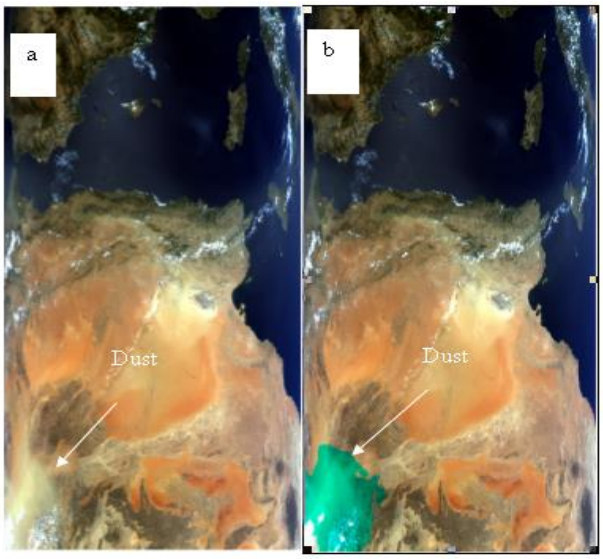

Figure 2 (a) is a true colour image of a dust storm over the Sahara desert (b) shows in green the region classified as dust storm by the trained neural network.

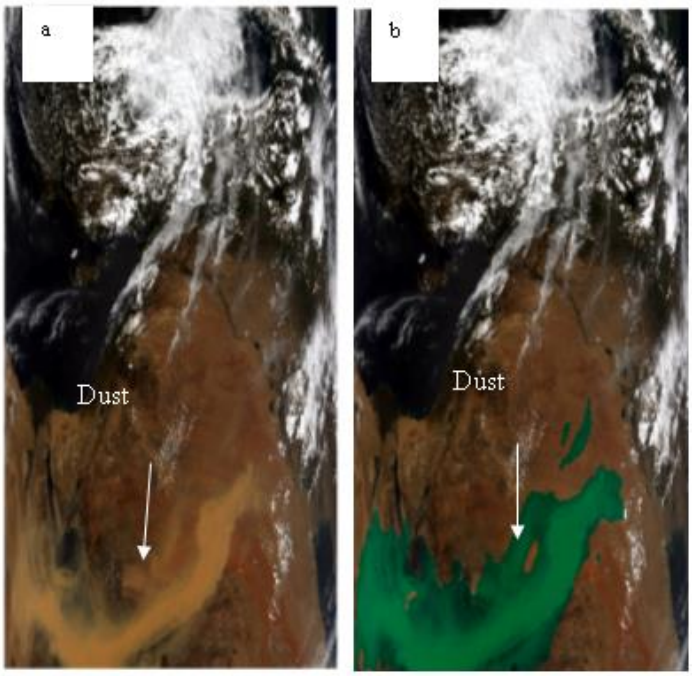

figure 3 (a) is a true colour image of a dust storm over northern Saudi Arabia (b) shows in green the region classified as dust storm by the trained neural network

B. Vegetation Surfaces Results :

To evaluate the performance of this technique for detecting dust storms over vegetation covered surfaces it was applied to data from China and Afghanistan where it was found to detect 88% of manually observed dust storms. Table IV illustrate the average result of detection dust storm over vegetation surfaces

table IV the result of trained neural network over vegetation surfaces.

	TPR	FPR	ACC	TNR	FDR
Average	0.85	0.10	0.90	0.90	0.70

Figure 4a shows a heavy dust storm on 11th of November 2010 over north eastern China captured by the Terra satellite. Figure

5a shows a heavy dust storm over northern Afghanistan on 5th of October 2011 captured by the Aqua satellite. Figures 4b and 5b illustrate the ability of the method to discriminate dust storm from vegetation surfaces and cloud.

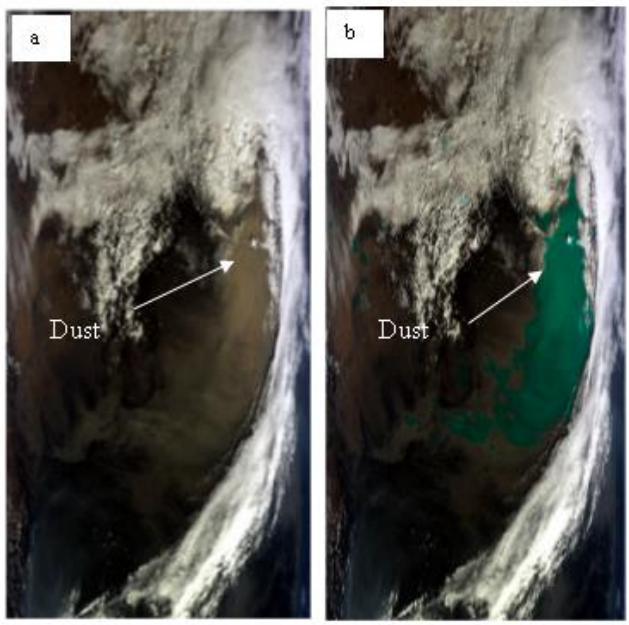

figure 4 (a) is a true colour image of a dust storm over north eastern china (b) shows in green the region classified as dust storm by the trained neural network.

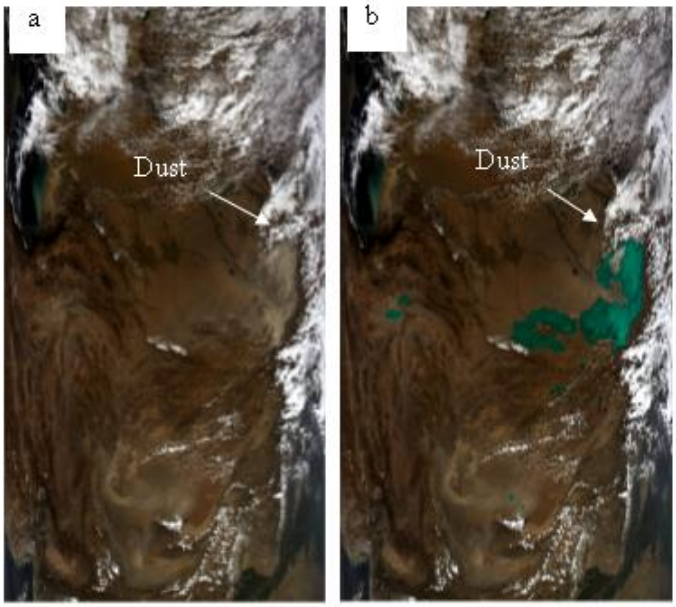

Figure 5 (a) is a true colour image of a dust storm over northern Afghanistan (b) shows in green the region classified as dust storm by the trained neural network.

C. Ocean surfaces :

To evaluate the performance of this technique for detecting dust storms over ocean surfaces it was applied to data from the North Atlantic where it was found to detect over all about 72% of manually observed dust storms pixels over sea and ocean surface. Table V illustrate the average result of detection dust storm over water surface.

table V the result of trained neural network over water surfaces.

	TPR	FPR	ACC	TNR	FDR
Average	0.72	0.06	0.91	0.94	0.40

The algorithm detects thick dust storm over water but some weaker dust storm is not detected. Figures 6a and 7a show true colour images of dust storms over the Atlantic Ocean on 12th of February 2005 captured by the Terra and Aqua satellites

respectively. Figures 6b and 7b illustrate the ability of the method to discriminate between dust storm and water. It can clearly be seen that some of the dust is not detected and that is because the temperature of ocean surface is lower than land and does not affected with weak dust storm. So the BTD of weak dust storm and ocean surface are similar. For this season, there is a need of finding a way to subtract the ocean surface before classification or probably the using of multiple classifications could be more affective for detection dust storms over ocean surface.

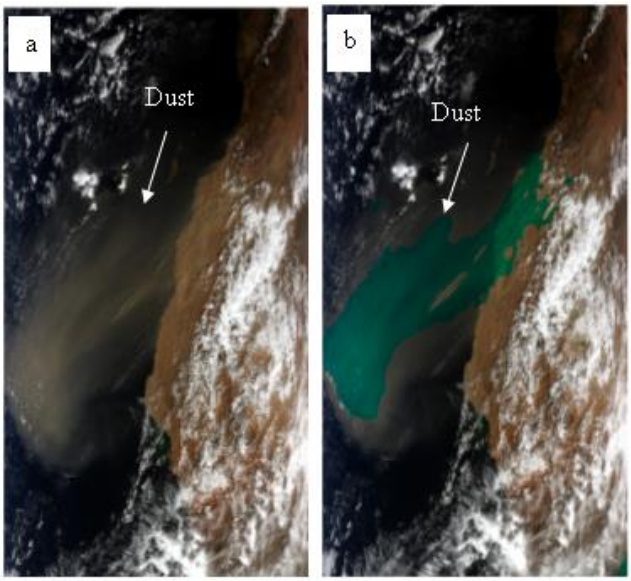

figure 6(a) is a true colour image a of a dust storm blown from the Sahara over the Atlantic ocean(b) shows in green the region classified as dust storm by the trained neural network .

D. Night Time :

To evaluate the performance of the algorithm to dust storms observed at night it was applied to data from Jordan and Saudi Arabia where it was found to detect over all 86% of manually observed dust storms pixels. Table VI illustrate the average result of detection dust storm during night over desert surface.

table VI the result of trained neural network over water surface.

	TPR	FPR	ACC	TNR	FDR
Average	0.86	0.10	0.89	0.89	0.60

Figures 8a and 9a show false colour images produced by the combination of bands 20, 31 and 32 where dust storms appear light purple in colour. Figure 8a show the beginning of a dust storm over the south of Jordan captured by the Aqua satellite on 12 of May 2005 at night time. Figure 9a shows the same dust storm on 13 of May 2005 moving to the south. A true colour image of this dust storm during the day is shown in Figure 3a. Figures 8b and 9b illustrate the ability of this algorithm to discriminate dust at night. Some of the weaker dust storm over water is missed.

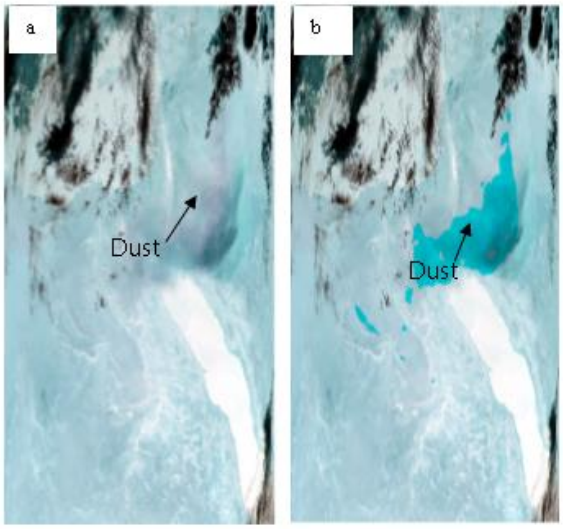

Figure 7 (a) is a false colour image of a dust storm over southern Jordan captured at night (b) shows in cyan the region classified as dust storm by the trained neural network.

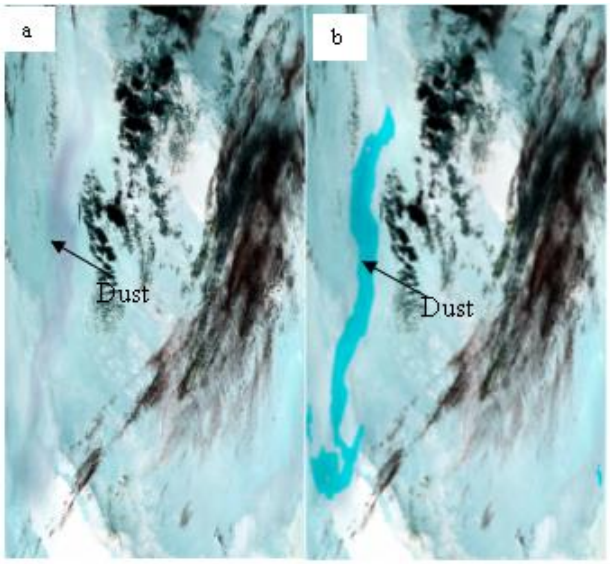

figure 8 (a) is a false colour image of the dust storm shown in figure 7 the next day when it is over northern Saudi Arabia (b) shows in cyan the region classified as dust storm by the trained neural network.

V. CONCLUSIONS AND FUTURE WORK :

In this study we demonstrate the application of a new dust storm detection approach, based on a neural network binary classifier with a feature vector comprising four brightness temperature differences and brightness temperature of band 31 calculated, using MODIS data from the Terra and Aqua satellites in bands 20, 23, 29, 31, and 32. The trained neural network was able to discriminate dust storms from cloud and desert land surfaces with similar characteristics with an accuracy of about 80% in the day and 86% at night. The detection accuracies over vegetation and water surfaces were about 85% and 72% respectively. This technique can detect weak and strong dust storms over both sandy and non sandy

surface for both day and night. However, the detection of weak dust storms over water surfaces during both day and night is the area which shows poorest performance. It is intended in future to develop the neural network approach by considering groups of pixels rather than individual pixels and with additional output classes including land, dust storm, vegetation, water and cloud instead of the binary classification dust or no-dust.

REFERENCES :

[1] J. J. Qu, et al., "Asian Dust Storm Monitoring Combining Terra and Aqua MODIS SRB Measurements," Geoscience and Remote Sensing Letters, IEEE, vol. 3, pp. 484-486, 2006.

[2] S.-c. Liu, et al., "Detection of Dust Storms by Using Daytime and Nighttime Multi-spectral MODIS Images," in Geoscience and Remote Sensing Symposium, 2006. IGARSS 2006. IEEE International Conference on, 2006, pp. 294-296.

[3] H. El-Askary, et al., "Introducing new approaches for dust storms detection using remote sensing technology," in Geoscience and Remote Sensing Symposium, 2003. IGARSS '03. Proceedings. 2003 IEEE International, 2003, pp. 2439-2441 vol.4.

[4] DI Mei, et al., "A Dust Storm Process Dynamic Monitoring WIith Multi-Temporal MODIS Data," The International Archives of the Photogrammetry, Remote Sensing and Spatial Information Sciences, vol. XXXVII. Part B7, pp. 965-970, 2008.

[5] W. Kaiping, et al., "Detection of Sand and Dust Storms from MERIS Image Using FE-Otsu Alogrithm," in Bioinformatics and Biomedical Engineering, 2008. ICBBE 2008. The 2nd International Conference on, 2008, pp. 3852-3855.

[6] T. Han, et al., "Automatic detection of dust storm in the northwest of China using decision tree classifier based on MODIS visible bands data," in Geoscience and Remote Sensing Symposium, 2005. IGARSS '05. Proceedings. 2005 IEEE International, 2005, pp. 3603-3606.

[7] O. S. Hansell R, Liou K, Roskovensky J, Tsay S, Hsu C, Ji Q, "Simultaneous detection/separation of mineral dust and cirrus clouds using MODIS thermal infrared window data," GEOPHYS RES LETT, vol. 34, p. 5, 2007 Jun 9 2007.

[8] L. Yang and L. Ronggao, "A thermal index from modis data for dust detection," in Geoscience and Remote Sensing Symposium (IGARSS), 2011 IEEE International, 2011, pp. 3783-3786.

[9] E. El-ossta, et al., "A New Approach for the Detection of Dust Storms Using Multi-spectral MODIS bands " presented at the Mosharaka International Conference on Communications, Computers and Applications Amman Jordan, 2009.

[10] P. Rivas-Perea, et al., "Traditional and neural probabilistic multispectral image processing for the dust aerosol detection problem," in Image Analysis & Interpretation (SSIAI), 2010 IEEE Southwest Symposium on, pp. 169-172.

[11] N. Iino, et al., "Detection of Asian dust aerosols using meteorological satellite data and suspended particulate matter concentrations," Atmospheric Environment, vol. 38, pp. 6999-7008, 2004.

[12] LAADS http://ladsweb.nascom.nasa.gov/data/search.html.